Author Manuscript

Sensitivity of Modeled Soil NOx Emissions to Soil Moisture

Daniel E. Huber, Allison L. Steiner, Eric A. Kort

Department of Climate and Space Sciences and Engineering, University of Michigan, Ann Arbor

Corresponding author: Daniel Huber (dehuber@umich.edu)

Key Points:

- A soil NOx emissions (S_{NOx}) parameterization is updated to reflect the dynamic spatial relationships between soil moisture and S_{NOx}.
- The updated parameterization produces consistent S_{NOx} estimates when using different soil moisture products to drive the model.
- Regions of the Eastern United States with intensively managed cropland experience the largest increases in S_{NOx}.

This is the author manuscript accepted for publication and has undergone full peer review but has not been through the copyediting, typesetting, pagination and proofreading process, which may lead to differences between this version and the Version of Record. Please cite this article as doi: 10.1029/2022JD037611.

This article is protected by copyright. All rights reserved.

Author Manuscript

Abstract

As emissions of nitrogen oxides (NOx) from fossil fuel combustion decrease, the relative contribution of NOx emissions from managed and unmanaged soils (S_{NOx}) is increasing. Modeling S_{NOx} presents a challenge as it requires proper characterization of emission dynamics in response to environmental conditions. S_{NOx} is often represented using the Berkeley Dalhousie Soil NOx Parameterization (BDSNP), which relies upon static relationships between soil moisture and S_{NOx} for arid and non-arid lands. However, soil chamber and atmospheric studies have shown that emission characteristics are more dynamic, with peak emissions often occurring at higher soil moisture content. Here, to better capture observational studies, we update BDSNP by creating a dynamic S_{NOx} response to soil moisture based on a normalized soil moisture index. We compare the standard and updated parameterizations over the contiguous United States (U.S.) for 2011-2020 using input soil moisture data from ERA5-Land, MERRA-2 and NLDAS2-Mosaic and evaluate S_{NOx} across these different input drivers as well as between the standard and updated parameterizations. The standard parametrization exhibits strong sensitivity to different input soil moisture products, with annual U.S. S_{NOx} differences of up to 0.28 Tg N yr^{-1}. In contrast, the updated parameterization provides a robust representation of S_{NOx} with reduced sensitivity to input soil moisture product with differences of at most 0.03 Tg N yr^{-1}. The updated parameterization simulates a broad increase in S_{NOx} in non-arid regions, including much of the Eastern U.S., indicating that this region may be more sensitive to climatically-driven S_{NOx} as anthropogenic NOx emissions continue to decline.

Plain Language Summary

Nitrogen oxides (NOx = NO + NO_2) are reactive nitrogen gases that have a direct negative impact on health and air quality. While most NOx in the United States derives from fossil fuel

This article is protected by copyright. All rights reserved.

combustion, a substantial fraction is released into the atmosphere by microbial processes in the soil. One frequently used model parameterization estimates soil NOx emissions from environmental factors including soil moisture, with a spatially constant relationship between soil NOx and soil moisture despite different soil and ecosystem characteristics. We update this model parameterization to produce variable soil moisture-NOx relationships for different locations based on local soil moisture history. Unlike the standard parameterization where emissions varied greatly with different soil moisture input datasets, the updated parameterization produces similar results regardless of the soil moisture dataset. The revised soil moisture relationship increases modeled soil NOx emissions over much of the intensively managed cropland across the eastern United States, with potential to influence local and regional air quality.

1. Introduction

Nitrogen oxides (NOx = NO + NO2) are direct air pollutants responsible for a range of negative health impacts and increased mortality (Forastiere and Peters, 2021). Beyond its direct health impacts, NOx also plays a crucial role in the formation of harmful secondary air pollutants, including ozone and particulate matter (Duncan et al., 2010; Hauglustaine et al., 2014). In the United States (U.S), fossil fuel combustion represents the largest source of NOx emissions, although fossil NOx emissions have been decreasing over the past two decades (Jiang et al., 2022). This decline in fossil NOx emissions has highlighted the increasing importance of other NOx sources, including soils, to the overall NOx budget (Miyazaki et al., 2020; Geddes et al., 2022). While soil NOx emissions (S_{NOx}) occur naturally in most soils, the most intense emissions are anthropogenic and occur in cropland regions where nitrogen-rich fertilizers are applied to soils (Almaraz et al., 2018). These anthropogenically-influenced emissions have local impacts (Lu et al., 2021). Biogenic S_{NOx} form the bulk of background NOx concentrations, particularly in rural

This article is protected by copyright. All rights reserved.

Author Manuscript

regions (Silvern et al., 2019). Given its growing importance to atmospheric NOx, improved understanding of processes controlling S_{NOx} is imperative for improving our understanding of the role of NOx in the formation of secondary air pollutants and its influence on air quality (Qu et al., 2021; Geddes et al., 2022).

Globally, soils are a significant source of NOx to the atmosphere, with the most recent global top-down satellite analysis estimating approximately 13 Tg of NOx-N emissions annually (Vinken et al., 2014), however other estimates ranging from 3.3 to 20.4 Tg of NOx-N have been reported (Weng et al., 2020). S_{NOx} are triggered by microbes within soil pore space which drive nitrification and denitrification, two processes largely responsible for the emission of nitric oxide (NO). Nitrification represents the oxidation of ammonium (NH_4^+) to nitrate (NO_3^-) while denitrification represents the reduction of NO_3^- to gaseous nitrogen (N_2); both processes can emit NO as a byproduct. Nitrification and denitrification are heavily influenced by environmental conditions, including soil moisture, soil temperature and soil nitrogen content, with emissions maximized at moderate soil moisture, high temperatures and high nitrogen content (Pilegaard, 2013). Soils can also emit NOx through a process known as soil NOx pulsing, during which a relatively short-lived but large amount of NO can be emitted (Eberwein et al. 2020). The typical definition of pulsing occurs when dry soil is rewetted at the end of a prolonged dry period, which induces a metabolic response from microbes within the soil, resulting in NO emissions that can be many times the magnitude of pre-pulsing emissions (Zörner et al., 2016).

Yienger and Levy (1995) developed one of the first S_{NOx} parameterizations which can be used in global atmospheric chemistry models, and estimates emissions using temperature, precipitation, fertilizer application, vegetation type, and canopy cover. The Yienger and Levy parameterization was expanded upon with the Berkeley-Dalhousie Soil NOx Parameterization (BDSNP), a widely-

This article is protected by copyright. All rights reserved.

Author Manuscript

used S_{NOx} parameterization that includes biome-specific emission coefficients and soil NOx pulsing (Hudman et al., 2012) and has been used in various chemical transport models, including GEOS-Chem, CMAQ and WRF-Chem (Hudman et al., 2012; Rasool et al., 2016; Sha et al., 2021). BDSNP represents S_{NOx} with four multiplicative terms:

$$S_{NOx} = A'_{biome}(N_{Avail}) \times f(T) \times g(WFPS) \times P(L_{dry}) \quad (1)$$

where A'_{biome} is the biome-dependent soil NOx emissions factor, which is a function of available soil nitrogen (N_{Avail}) and a wet biome emissions coefficient from Steinkamp and Lawrence (2011), f(T) is an exponential soil temperature function and g(WFPS) is a Poisson function which scales emissions from 0 to 1 based on water-filled pore space (WFPS) and climate (arid vs. non-arid) at each location. Pulsed emissions are represented in Eq. 1 with $P(L_{dry})$, a function of the length of the preceding dry period and time since pulse was initiated. In this parameterization, g(WFPS) peaks at 20% WFPS in arid regions and at 30% WFPS in non-arid regions.

Soil moisture is a particularly powerful control on S_{NOx}, as soil moisture regulates the amount of air in the soil pore space, where microbes responsible for nitrification and denitrification require varying amounts of oxygen to remain active (Davidson ., 1993). For this reason, WFPS is a useful metric to estimate the relative magnitude of S_{NOx}. WFPS is defined as:

$$\text{WFPS} = \frac{\text{VSM}}{\text{P}} \quad (2)$$

where VSM is the volumetric soil moisture and P is the soil porosity. The influence of soil moisture on S_{NOx} is inferred from a combination of previous field and laboratory chamber studies investigating soil nitrogen content, soil microbial activity and fluxes of NOx from soils. These studies indicate that S_{NOx} are typically low at very wet or very dry conditions, and greatest at a moderate WFPS. However, the WFPS where S_{NOx} peaks has been observed at a range of different

This article is protected by copyright. All rights reserved.

Author Manuscript

values. In a S_{NOx} chamber study in Southern California, U.S., Oikawa et al. (2015) identified peak S_{NOx} at an optimum of approximately 30% VSM, or approximately 60% WFPS, depending on the assumed soil porosity. Huang et al. (2022) found S_{NOx} to peak at 37% WFPS during the growing season in a chamber study in Northeastern China. Schindlbacher and Zechmeister-Boltenstern (2004) investigated S_{NOx} at various forested sites in Europe and found the soil moisture optimum for S_{NOx} to range from 15% – 65% WFPS, depending on the location. In a previous study (Huber et al., 2020), we utilized space-based NO_2 observations from the Tropospheric Monitoring Instrument (TROPOMI) and space-based soil moisture observations from Soil Moisture Active Passive (SMAP) to identify peak S_{NOx} at approximately 65% WFPS in a cropland region in Mississippi, U.S. Numerous other studies have shown that S_{NOx} can peak at drier soil conditions less than 50% WFPS (Maljanen et al., 2007; Schaufler et al., 2010; Szukics et al., 2010; Laville et al., 2011; Su et al., 2021) as well as in wetter soil conditions greater than 50% WFPS (Gasche & Papen, 1999; Yao et al., 2010; Zhou et al., 2010; Hall et al., 2018; Mushinski et al., 2020; Ke et al., 2021). This range of observed WFPS values for peak S_{NOx} could be due to several confounding environmental factors, including the adaptation of soil microbes to wet or dry conditions (van Dijk & Duyzer, 1999), or the relationship of current soil moisture to field capacity at individual locations (Davidson et al., 1993; Schaufler et al., 2010).

Previous studies have modified the BDSNP to include more detailed processes as more observations of S_{NOx} become available. Sha et al. (2021) updated the standard static representation of arid vs. non-arid land to allow the classification to vary in time, producing emissions over California that were in better agreement with satellite NO_2 observations. Wang et al. (2021) updated the temperature dependence function (f(T) in Equation 1) based on field observations from

This article is protected by copyright. All rights reserved.

Author Manuscript

Oikawa et al. (2015), which increased S_{NOx} at higher temperatures relative to the standard function and led to an 18.2% increase in S_{NOx} over the U.S.

In this study, we introduce an updated BDSNP parameterization for S_{NOx} focusing on soil moisture controls to improve the representation of soil moisture on S_{NOx}. Soil moisture can be derived from observations or model simulations, and it is a particularly challenging quantity to represent accurately given its strong spatial heterogeneity and sparse in situ observations. We evaluate the role of soil moisture on the parameterization of S_{NOx} used within many atmospheric chemistry models to understand the sensitivities of emissions estimates to the treatment of this physical relationship. We update the BDSNP soil moisture function by designing S_{NOx} to peak at the median spring-summer soil moisture value at each grid cell, creating a more dynamic representation than the arid vs. non-arid classification approach currently used. We further update the soil moisture threshold within the pulsing function that defines the presence of a dry period. We run the BDSNP for the contiguous U.S for 2011-2020 with the standard and updated parameterization using meteorological input data from 3 different sources to compare emission estimates driven by different gridded soil moisture products. We show that, while retaining the overall sensitivity to soil moisture, our updated scheme makes emission estimates more consistent regardless of the choice of soil moisture input, with the updated parametrization producing larger S_{NOx} across much of the eastern U.S. than the standard scheme.

2. Updated BDSNP parameterizations

2.1. Soil Moisture Definitions

Soil moisture can be defined in several ways, including as (1) volumetric soil moisture (VSM; $cm^3\ cm^{-3}$) representing the volume of water per volume of soil and (2) water-filled pore space (WFPS; $cm^3\ cm^{-3}$) which is the VSM divided by the soil porosity (Equation 2). Climate based soil

This article is protected by copyright. All rights reserved.

Author Manuscript

moisture observations, Earth system models and atmospheric/land reanalysis products typically utilize the VSM definition (Li et al., 2020), while most S_{NOx} studies use WFPS, which is a more relevant parameter for soil NOx and microbial activity. For both models and observations, there can be large variations in soil moisture depending on the data source (Beck et al., 2021), in addition to the strong heterogeneity in soil moisture across soil and ecosystem gradients (Famiglietti et al., 2008).

To better represent the spatial heterogeneity of wet and dry soil moisture regimes, we normalize soil moisture to local grid cell values, which we refer to as normalized volumetric soil moisture (NVSM):

$$\mathrm{NVSM(t)} = \frac{\mathrm{VSM(t)} - \mathrm{VSM_{min}}}{\mathrm{VSM_{max}} - \mathrm{VSM_{min}}} \quad (3)$$

where at each grid cell, $\mathrm{VSM(t)}$ is the VSM at time t, $\mathrm{VSM_{min}}$ is the minimum VSM for a ten year period and $\mathrm{VSM_{max}}$ is the maximum VSM for a ten year period. At each grid cell, NVSM ranges from 0 to 1, where 0 is the driest and 1 is the wettest observed condition at that location. This provides a measure of how wet or dry a given location is relative to its modeled soil moisture history. We calculate NVSM for each grid cell and for each soil moisture product individually. This normalized approach to soil moisture is representative of S_{NOx} as observed in previous studies (Ke et al., 2021).

2.2. Arid and semi-arid classifications

The standard BDSNP classifies each pixel as either arid (including both arid and semi-arid land cover classifications) or non-arid to determine the WFPS of peak S_{NOx}. Arid and semi-arid pixels experience peak emissions at 20% WFPS, while non-arid pixels experience peak emissions at 30% WFPS (Hudman et al., 2012). Areas receiving less than 25 centimeters (cm) of rain

This article is protected by copyright. All rights reserved.

Author Manuscript

annually are classified as arid, areas receiving between 25 and 50 cm of rain annually are classified as semi-arid, and areas receiving more than 50 cm of rain annually are classified as non-arid (Jafari et al., 2018). By this definition, most of the western half of the contiguous U.S. is classified as arid or semi-arid, while most of the eastern half is classified as non-arid. Because the updated soil moisture function (sec. 2.3) is dependent on local soil moisture history, we no longer consider the arid vs. non-arid classification in the updated parameterization.

2.3. Revised BDSNP Soil Moisture Function

The standard BDSNP soil moisture function in Equation 1 is represented by a Poisson function of WFPS (Fig. 1a) that increases S_{NOx} with increasing soil moisture until an optimum WFPS is reached, after which S_{NOx} decreases with increasing soil moisture:

$$g(WFPS) = a * (WFPS) * exp(-b * WFPS^c) \quad (4)$$

where coefficients a, b and c define a curve that peaks (g(WFPS)=1) at the WFPS optimum. In the standard BDSNP, there are two possible soil moisture optima at which g(WFPS) = 1: at 20% WFPS if a pixel is classified as arid **(**a=8.25, b=12.5, and c=2) and at 30% WFPS if a pixel is classified as non-arid (a=5.5, b=5.55, and c=2). As WFPS diverges from these optima (i.e. soils become wetter or drier), the value of g(WFPS) decreases, which subsequently scales emissions lower (Fig. 1a). We have updated this function as explained in the following subsections.

2.3.1. Use of Normalized Volumetric Soil Moisture (NVSM)

The standard BDSNP soil moisture term produces lowest emissions at low and high values of WFPS (Figure 1a). However, due to the strong heterogeneity of soil moisture, a WFPS value that may be considered dry in one region (e.g. 40% WFPS in parts of the eastern U.S. summer) can translate into a WFPS value that may considered quite wet in a different region (e.g. 40% WFPS

This article is protected by copyright. All rights reserved.

Author Manuscript

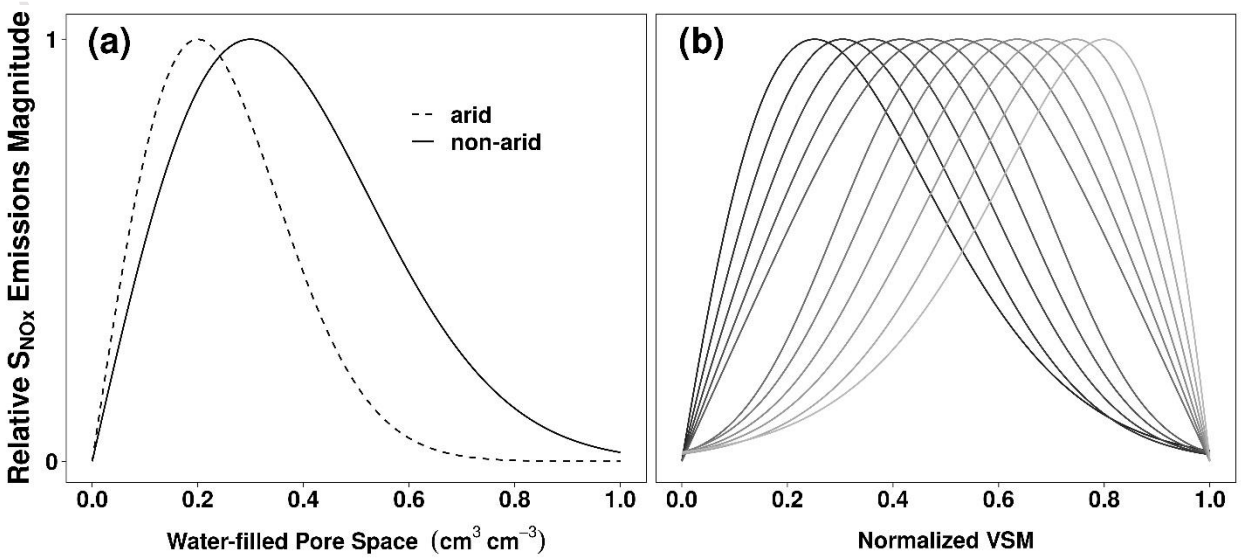


Figure 1: (a) Standard BDSNP soil moisture functions, which produce peak emissions at 20% WFPS in arid regions and at 30% WFPS in non-arid regions. (b) Updated BDSNP soil moisture functions, which produce peak emissions at the median normalized volumetric soil moisture (NVSM) for April-September. Each curve represents a conceptual soil moisture function that changes for each grid cell. Spatial representation of 1B is shown in Figures 4d-f.

in parts of the western U.S. summer), yet the standard BDSNP soil moisture function would scale the NOx emissions at those locations in the same manner. This could lead to an overestimation of S_{NOx} when soils within a specific region are likely too wet or too dry to produce high emissions. In the revised parameterization, we use NVSM as the soil moisture metric (Sec. 2.1), which allows for a more realistic comparison between the relative wet or dry status of different regions, which is not always possible when using WFPS.

2.3.2. Soil NOx Maximum at Median NVSM

The standard BDSNP provides two soil moisture regimes for peak S_{NOx}, with largest emissions occurring at 20% and 30% WFPS in arid and non-arid regions, respectively (Figure 1a). While this produces peak emissions at moderate soil moisture values, the specific WFPS of peak S_{NOx} has been observed to be much more dynamic across a range of soils and ecosystems (Schaufler et al., 2010; Hall et al., 2018). To allow for spatially dynamic soil moisture optima for peak S_{NOx} with location specific soil moisture ranges, the revised parameterization maximizes emissions at the

This article is protected by copyright. All rights reserved.

Author Manuscript

median NVSM for each grid cell. This approach produces peak emissions at moderate soil moisture conditions, without incorporating additional uncertainty associated with choosing a fixed soil moisture value for peak emissions across broad regions. This approach also removes uncertainty associated with soil porosity, which is needed to obtain WFPS. Further, the median soil moisture value is typically reached during soil drydown following precipitation, periods during which S_{NOx} have been observed to peak (Su et al., 2021; Andrews et al. 2022).

2.3.3. Coefficient Optimization

We optimize the coefficients of the standard soil moisture function (Eq. 4; coefficients a-c) to produce peak emissions (g(NVSM) = 1) at the grid cell's median NVSM, and low emissions at the wettest or driest conditions (g(WFPS) = 0).

$$g(NVSM) = \begin{cases} a \times NVSM \times \exp(-\mathrm{b} \times NVSM^{c}), & median\ NVSM < 0.5 \quad (5) \\ a \times (1 - NVSM) \times \exp(-b \times (1 - NVSM)^{c}), & median\ NVSM \geq 0.5 \quad (6) \end{cases}$$

In Equations 4-6, *c* determines the width of the response function, *b* sets the soil moisture value for the localized maxima, and *a* determines the amplitude of the localized maxima. We select *a*, *b* and *c* to result in near-zero emissions at the lower and upper bounds of NVSM=0 and NVSM=1 and a normalized value of g(NVSM)=1 at the median NVSM at each grid cell. For a given median NVSM value, we achieve this by first holding *a* constant and iteratively testing different combinations of *b* and *c* to identify the combination that produces (1) a local maximum at the median NVSM and (2) near zero emissions at the upper at lower NVSM bounds. Once the values of *b* and *c* have been solved for, they are put into Eq. 5 or Eq. 6, and *a* is then solved for when g(NVSM) = 1. This process is repeated for each median NVSM value to determine the unique combination of *a*, *b* and *c* for each soil moisture optimum. A visual representation of possible curves is shown in Figure 1b, where regions of the Western U.S. will typically have a median

This article is protected by copyright. All rights reserved.

Author Manuscript

NVSM value that falls within the lower 50% of the range (darker curves) and Eastern U.S. regions typically have a median NVSM that falls within the upper 50% of the range (lighter curves).

2.3.4. Irrigation Adjustment

Most modeled soil moisture products do not account for irrigation. In irrigated regions of the Western U.S. that often receive little to no summertime rainfall, soil moisture products estimate very dry soils during the summer, even though regular summertime irrigation is occurring. As a result, irrigated grid cells likely experience higher soil moisture during the summer than the models predict (Zaussinger et al., 2019). If irrigation is not accounted for and modeled soil moisture in irrigated regions remains very dry during the summer, then the updated S_{NOx} estimates in Western U.S. cropland regions are reduced to unrealistically low values.

To address this discrepancy, we use the Moderate Resolution Imaging Spectroradiometer (MODIS) Irrigated Agriculture Dataset (MIrAD-US) from Pervez and Brown (2010), which provides an estimate of the irrigated percentage of land at 250 m spatial resolution for the U.S. Using this dataset, we identify grid cells west of 100 degrees longitude with greater than 50% irrigation, and assume that soil moisture is fixed at the 15th percentile of the NVSM range in those regions during April-September. This value was chosen to ensure that NVSM is not near zero for the summer months when S_{NOx} are known to be largest, but still keeps soil moisture within the drier range of values on average. This adjustment only impacts a small number of grid cells, primarily limited to portions of California, Idaho and Washington State.

2.4. Revised soil moisture thresholds for soil NOx pulsing function

In the standard BDSNP parameterization (Eq. 1), soil NOx pulsing is a function of the length of the dry period prior to rainfall and time since the pulse began.

This article is protected by copyright. All rights reserved.

Author Manuscript

$$P\left(l_{dry}, \mathrm{t}\right) = \left[13.01 \ln\left(l_{dry}\right) - 53.6\right] \times e^{-0.068 \times t} \quad (7)$$

In Eq. 7, the length of the dry period (l_{dry}) is defined as the length of time in hours that VSM has been below a threshold of 17.5% (Hudman et al., 2012). A threshold value is used to ensure that soils are sufficiently dry for microbes to be in a mostly inactive state. If VSM lies below this threshold and soils are rewetted to significantly increase VSM, then the metabolic activity of the microbes is assumed to increase rapidly, leading to a short-lived (1-2 day) pulse of NO from the soil. However, the soil moisture threshold that defines a dry period remains poorly defined, and depending on the soil moisture product being used, soils will dry to below this threshold at varying levels of frequency. Further, using VSM as the soil moisture metric to define the threshold results in multiple soil moisture metrics being used within the BDSNP, as the soil moisture dependence function is already a function of WFPS.

We use NVSM to define the threshold for soil NOx pulsing to consistently use only one soil moisture metric for both the soil moisture dependence function (Equations 5 & 6) and the pulsing function (Equation 7). In most dry, arid regions, the median NVSM for all three soil moisture products falls below 0.33 NVSM. For grid cells with median NVSM less than 0.33, we define the pulsing threshold at the median NVSM value, meaning NVSM must remain below the median NVSM until soils are wetted again in order for a pulse to occur. For grid cells where median NVSM is typically greater than 0.33, we fix the pulsing threshold at 0.33 NVSM. By fixing the maximum pulsing threshold at 0.33 NVSM, we ensure that pulsing is mostly induced in drier climates. This approach allows the pulsing threshold to be tailored to the range of observed values for each soil moisture product and at each grid cell, as opposed to using one fixed value for the threshold at all locations and for all soil moisture products.

This article is protected by copyright. All rights reserved.

Author Manuscript

2.5. Monte Carlo Uncertainty Analysis

We quantify uncertainty in our emissions estimates using Monte Carlo simulations with 1000 iterations to propagate uncertainty from the input variables to uncertainty in our final emissions estimates. Given that uncertainty or error associated with the model input data (e.g. soil nitrogen, soil temperature and soil moisture) are not provided, we assume that for each iteration of the Monte Carlo simulation, the input data vary within ±5% of that variable's range at each grid cell for 2011-2020. For example, if the range of temperature values at one grid cell for the 2011-2020 period is 40 degrees Celsius, then the temperature T at time t at that grid cell will be perturbed to some value between T(t) ± 2 degrees C for each iteration of the Monte Carlo simulation. Perturbing each input variable in this way before quantifying emissions results in a sampling distribution of 1000 emissions estimates, from which we calculate a 95% confidence interval using the 2.5th and 97.5th percentile of the distribution as the lower and upper bounds of the interval.

We also consider the spatial correlation of input variables, as many input variables are correlated with each other spatially. We account for spatial correlation by applying a sinusoidal scaling function that perturbs the input variables gradually in space for each iteration, as opposed to perturbing each value randomly in space. Further, the wavelength of the sinusoidal scaling function used to scale each variable is changed for each iteration of the Monte Carlo simulation to some value between 150 kilometers (~6 grid cells) and 15000 kilometers (~600 grid cells) to account for unknowns in the correlation length scale of each variable.

3. Data

3.1. Soil Moisture and Temperature

This article is protected by copyright. All rights reserved.

Author Manuscript

We simulate S_{NOx} emissions with the standard and updated BDSNP using hourly gridded soil moisture and temperature data to drive the environmental functions in Equations 1-7. Because soil moisture products are variable (Li et al., 2020), we utilize soil moisture products from three reanalysis datasets: ERA5-Land (Muñoz-Sabater et al., 2021), MERRA-2 (Gelaro et al., 2017) and NLDAS2-Mosaic (Koster and Suarez, 1992). The products have native spatial resolution of 9 km x 9 km, 0.5° x 0.625° and 0.125° x 0.125°, respectively. We utilize the model soil layer closest to the surface, which varies slightly for each modeled product. For ERA5-Land, MERRA-2 and Mosaic, the surface layers correspond to depths of 0-7 cm, 0-5 cm and 0-10 cm, respectively. ERA5-Land and Mosaic are both land data assimilation systems, with ERA5-Land produced by the European Centre for Medium-Range Weather Forecasts (ECMWF) and Mosaic produced by the National Aeronautics and Space Administration (NASA). MERRA-2 is a coupled land-atmosphere reanalysis system also produced by NASA. All products are regridded to a 0.25° x 0.25° spatial resolution for model runs over the contiguous U.S. (Figure 2).

We obtain surface observations of volumetric soil moisture from the United States Climate Reference Network (USCRN) and the Soil Climate Analysis Network (SCAN) (Bell et al., 2013; Schaefer et al., 2007). Both networks provide observations from a variety of different locations, ranging from forested to agricultural. For this study we have chosen three SCAN sites and two USCRN sites within close proximity to cropland regions across the U.S. for comparison with modeled soil moisture estimates. The SCAN sites are located in Texas (station ID# 2106), Nebraska (station ID# 2001) and Ohio (station ID# 2014). The USCRN sites are located in Oregon (station WBAN# 04236) and Georgia (station WBAN# 63829). USCRN sites provide volumetric soil moisture estimates at depths of 5, 10, 20, 50 and 100 cm. SCAN sites provide volumetric soil moisture estimates at depths of 2, 4, 8, 20 and 40 inches. To evaluate these observations against

This article is protected by copyright. All rights reserved.

Author Manuscript

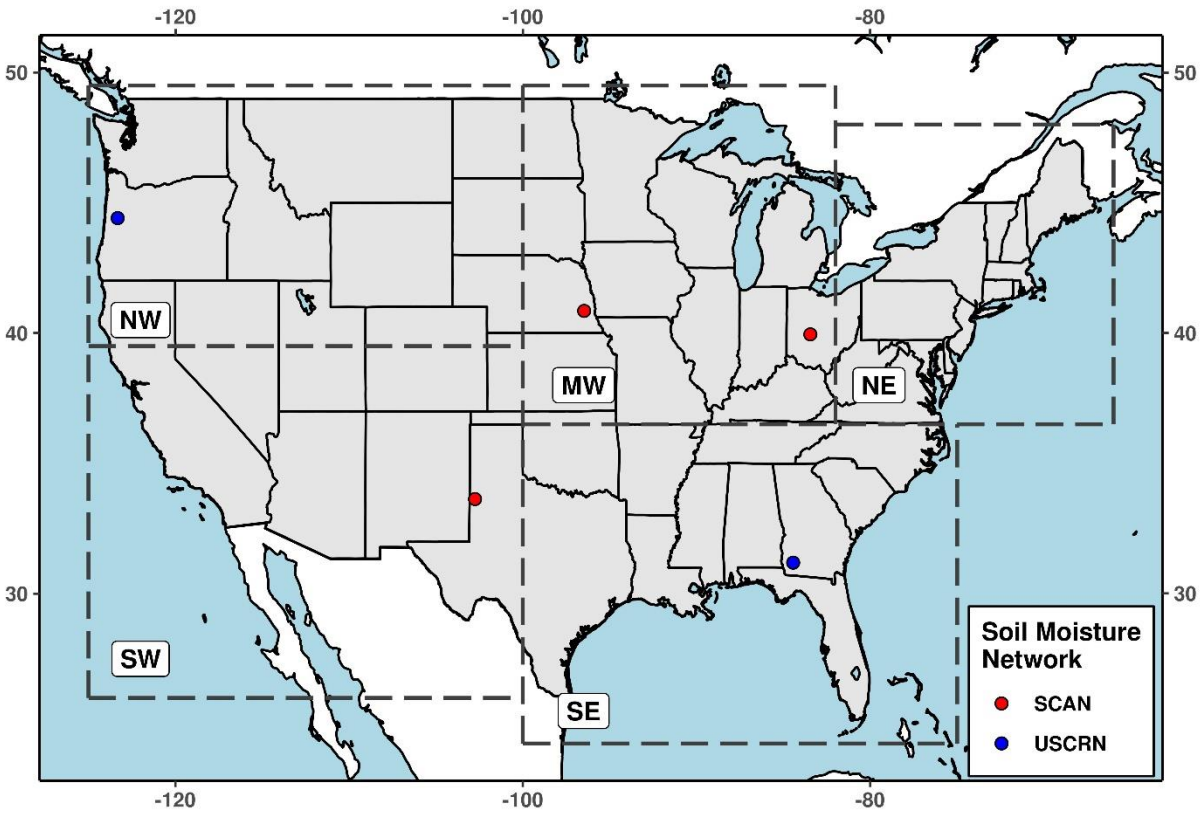


Figure 2: Contiguous U.S. model domain with regional domains for the northwest (NW), southwest (SW), Midwest (MW), northeast (NE), and southeast (SE). Red and blue points represent soil moisture network observations for select sites near agricultural regions.

the modeled soil moisture products used in this study, we use the top most soil layer from both networks of 0-5 cm and 0-2 inches. USCRN data can be accessed through the National Center for Environmental Information (https://www.ncei.noaa.gov/access/crn/qcdatasets.html) and SCAN data can be accessed through the National Resources Conservation Service (https://www.nrcs.usda.gov/wps/portal/wcc/home/quicklinks/).

3.2. Soil Porosity

Soil porosity is required to convert VSM to WFPS, with WFPS defined by the ratio of VSM to soil porosity (Eq. 2). We use soil porosity from the Catchment model provided with SMAP Level 4 modeled data (Reichle et al., 2017), which provides soil porosity on a 9km EASE grid which we regrid to the 0.25 degree grid for use within our study. We chose this soil porosity dataset

This article is protected by copyright. All rights reserved.

Author Manuscript

due to the high level of spatial heterogeneity included in the data, which results in a wider range of porosity values than is seen in other porosity datasets, e.g. porosity provided by MERRA-2.

3.3. Soil Nitrogen Availability

We use the TREND-nitrogen dataset (Byrnes et al., 2020) to represent available soil nitrogen (N_{Avail}; Equation 1). TREND-nitrogen separates sources and sinks of nitrogen, allowing for a mass balance approach to determine nitrogen concentrations within the soil. Sources of nitrogen include fertilizer, manure, deposition, biological nitrogen fixation and human waste, and sinks include crop uptake. For this study, we have omitted the human waste component, which is largest in large population centers. Because the dataset provides annual sums only, we assume a seasonal distribution of soil nitrogen as described in Hudman et al. (2012), where 75% of fertilizer is applied during the first month of the growing season, and the remaining 25% applied during the subsequent four months. Fertilizer N is assumed to have a soil lifetime of four months, while deposition N is assigned a lifetime of six months. The data are provided at the county level, and we use oversampling to convert the county level data to a 0.25 degree grid. This involves overlaying a fine resolution (0.05 degree) grid over the coarser county level data and disaggregating the county-level data to the smaller grid. The new 0.05 degree grid can then be averaged to the 0.25 degree grid used in our study. Data are provided annually until 2017, so we repeat 2017 data for our 2018-2020 model simulations.

4. Results

4.1. Soil Moisture Product Analysis

This article is protected by copyright. All rights reserved.

Author Manuscript

Because soil moisture is an important input to the calculation of S_{NOx}, we first evaluate the variations between the three modeled soil moisture products (Figure 3) over five regions of the US (defined in Figure 2). The 20% and 30% WFPS optima that define peak emissions in the standard BDSNP (see Section 2.1) typically fall within the interquartile range of WFPS in the northwest

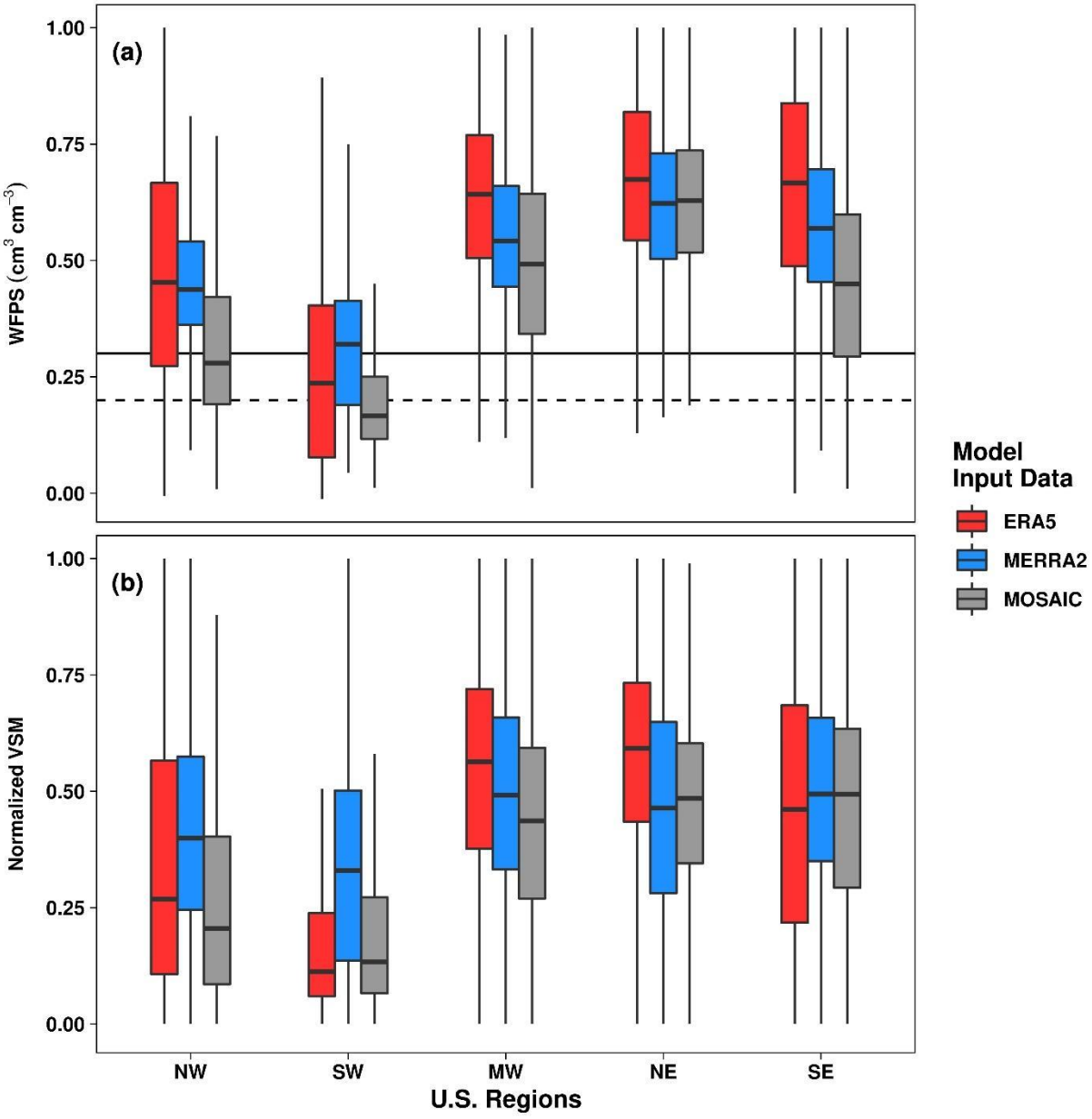


Figure 3: Regional soil moisture distributions for the growing season (April-September) in 2011-2020 for the three input soil moisture datasets (ERA5-Land in red, MERRA-2 in blue, and Mosaic in grey) represented as (a) WFPS (cm3 cm-3) and (b) normalized VSM (unitless). The dashed and solid horizontal black lines in (a) represent the WFPS of peak soil NOx emissions as used in the standard BDSNP for arid and non-arid regions, respectively.

This article is protected by copyright. All rights reserved.

Author Manuscript

(NW) and southwest (SW) regions (20-65% and 15-40% WFPS, respectively), indicating that emissions from the standard parameterization would frequently reach their maximum potential in these regions. In contrast, the range of WFPS values is higher (typically between 40-65% WFPS) in the Midwest (MW), northeast (NE) and southeast (SE) regions, indicating that the WFPS optima in the standard BDSNP occur less frequently in the eastern U.S. (Figure 3a). Further, most regions never approach 0% or 100% WFPS, even when at the relative wettest or driest conditions for a region. Therefore, emissions are rarely reduced to very low values, even during periods when conditions may be experiencing extreme wet or dry conditions when soil NOx emissions likely would be much lower. The use of NVSM does not substantially change the spatial soil moisture (i.e., drier in the west, wetter in the east), but it does allow a broader range of soil moisture values from wet to dry (Figure 3b).

To evaluate the WFPS and NVSM soil moisture input, we compare the three reanalysis products with select SCAN or USCRN soil moisture sites across the U.S. during the spring-summer that span a range of dry to wet conditions. Modeled soil moisture data represent the distribution of values from the regridded pixel closest to the respective SCAN or USCRN site. The distribution of WFPS observations for each soil moisture product and at each site show varying levels of agreement (Fig. 4, left column). At USCRN site #63829 in southern Georgia, the in situ observations and Mosaic are below 40% WFPS, while the distributions from ERA5-Land and MERRA-2 predominantly fall above 40% WFPS (Fig. 4a). At USCRN site #04236 near Corvallis, Oregon, all soil moisture products produce a bimodal soil moisture distribution, however the range of observed and modeled soil moisture values differ, with the peak of the driest mode ranging from 20% to 40% WFPS (Fig. 4c). At SCAN sites #2001 and #2014 in Nebraska and central Ohio,

This article is protected by copyright. All rights reserved.

Author Manuscript

Author Manuscript

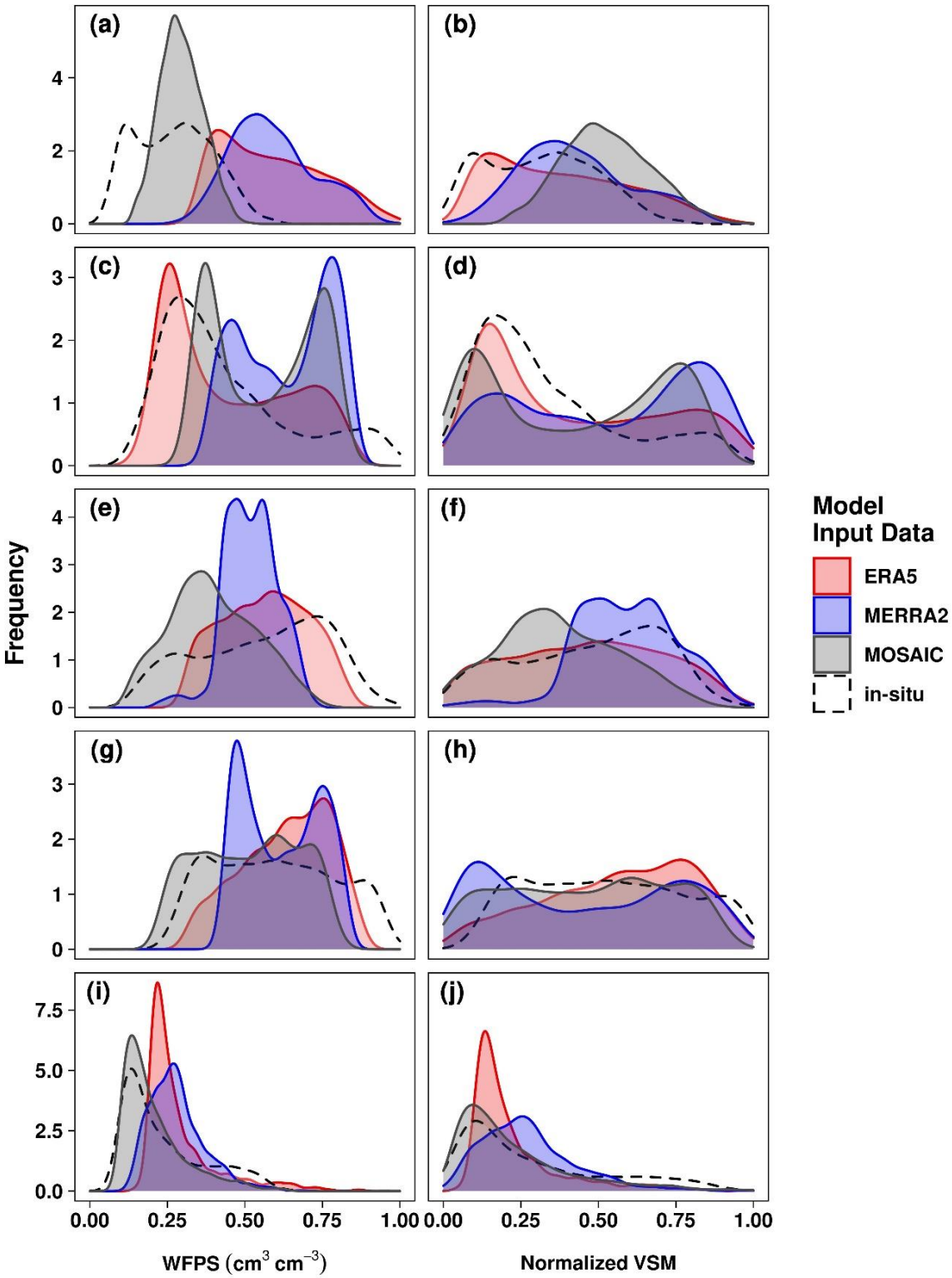


Figure 4: Soil moisture distributions for April-September at various soil moisture network sites across the U.S. in terms of WFPS (left) and normalized VSM (right). Distributions are shown for individual sites in Georgia (a-b), Oregon (c-d), Nebraska (e-f), Ohio (g-h) and Texas (i-j). Data from the three modeled products are taken from the grid cell nearest the observation site.

This article is protected by copyright. All rights reserved.

respectively, the observations show frequencies across the WFPS spectrum, whereas MERRA-2 soil moisture occurs over a moderate range of soil moisture (25% -75% WFPS) and the ERA5-Land biases wet and Mosaic biases dry. At SCAN site #2106 in Texas (Figure 4i), observations peak at low WFPS (~15%), which is matched by Mosaic and biased slightly wet in ERA5-Land and MERRA-2. After normalization (Figure 4, right column), the distribution of soil moisture between the different products and the observed soil moisture are in closer agreement. One exception is at the Oregon site, where the two products (Mosaic and MERRA-2) simulate a higher wet frequency (Fig. 4d). Normalizing the data does not always improve agreement between products, as can be seen at a site in central Texas (Fig. 4i-j) where agreement between soil moisture products before and after normalization remains relatively unchanged. However, for most locations, the normalized soil moisture products create a more consistent distribution of soil moisture as compared to observations, which in turn can help to create more consistent S_{NOx} estimates when used as inputs for the BDSNP.

The differences between the soil moisture data products also has implications for the simulation of soil NOx. For example, the ERA5-Land soil moisture product has been shown to exhibit a wet bias, including in the eastern U.S. and China (Wu et al., 2021; Xu et al., 2021; Li et al., 2020) and in the Midwestern U.S. (Figure 4e and 4g). In the eastern U.S., which is mostly classified as non-arid, the wet ERA5-Land bias translates into soil moisture values that are frequently higher than the 30% WFPS S_{NOx} optimum, and in many instances, soils are never dry enough for the emissions optimum to be achieved.

NVSM values more regularly reach the wettest and driest possible conditions (1 and 0, respectively), ensuring a reduction of emissions during these soil moisture extremes (Fig. 3b). Further, there is a general convergence in the NVSM range of the three data products, particularly

This article is protected by copyright. All rights reserved.

Author Manuscript

in the MW, NE and SE regions. For this soil moisture metric, the explicit arid and non-arid soil moisture optima no longer apply for the BDSNP soil moisture function, and emissions peak at the spring-summer median soil moisture value for each grid cell. In most cases, that translates into emissions peaking at wetter soil moisture conditions than in the standard parameterization, particularly in the eastern U.S. In the Eastern U.S., where the standard BDSNP parameterization produces peak emissions at 30% WFPS, updated emissions typically peak between 40% and 70% WFPS (Figure 5 d,e,f). In the Western U.S., where the standard BDSNP produces peak emissions at 20% WFPS, the WFPS of peak emissions remains minimally changed for the ERA5-Land and Mosaic products (Figure 5 d,f), but emissions now peak at notably higher soil moisture conditions for the MERRA-2 product, typically within the range of 35-45% WFPS (Figure 5e). Figures 5g-i show the growing-season average VSM for each product, before dividing by porosity to derive WFPS. In most forested regions in the Eastern U.S., ERA5-Land VSM is substantially higher than MERRA-2 or Mosaic VSM, which results in the updated S_{NOx} peaking at wetter soil conditions than MERRA-2 or Mosaic when using the ERA5-Land product to drive the model.

4.2. Annually-averaged Soil NOx Emissions: Standard vs. Updated Parameterization

We compare simulated soil NOx emission rates for the contiguous U.S. from 2011-2020 when using the standard and updated BDSNP parameterizations (Figure 6). Relative to the standard parameterization, the updated parameterization increases average contiguous U.S. S_{NOx} by 37.3% and 20.5% when driven by ERA5-Land and MERRA-2, respectively, and decreases contiguous U.S. S_{NOx} by 5.4% when driven by NLDAS-2 Mosaic. Regionally, the largest increase in emissions occur in broad sections of the eastern U.S. This includes the agriculturally-productive MW and SE regions where the multi-model average emissions increase by 18.8% and 18.4%, respectively, with the multi-model average being the mean S_{NOx} when using different soil moisture to drive the

This article is protected by copyright. All rights reserved.

Author Manuscript

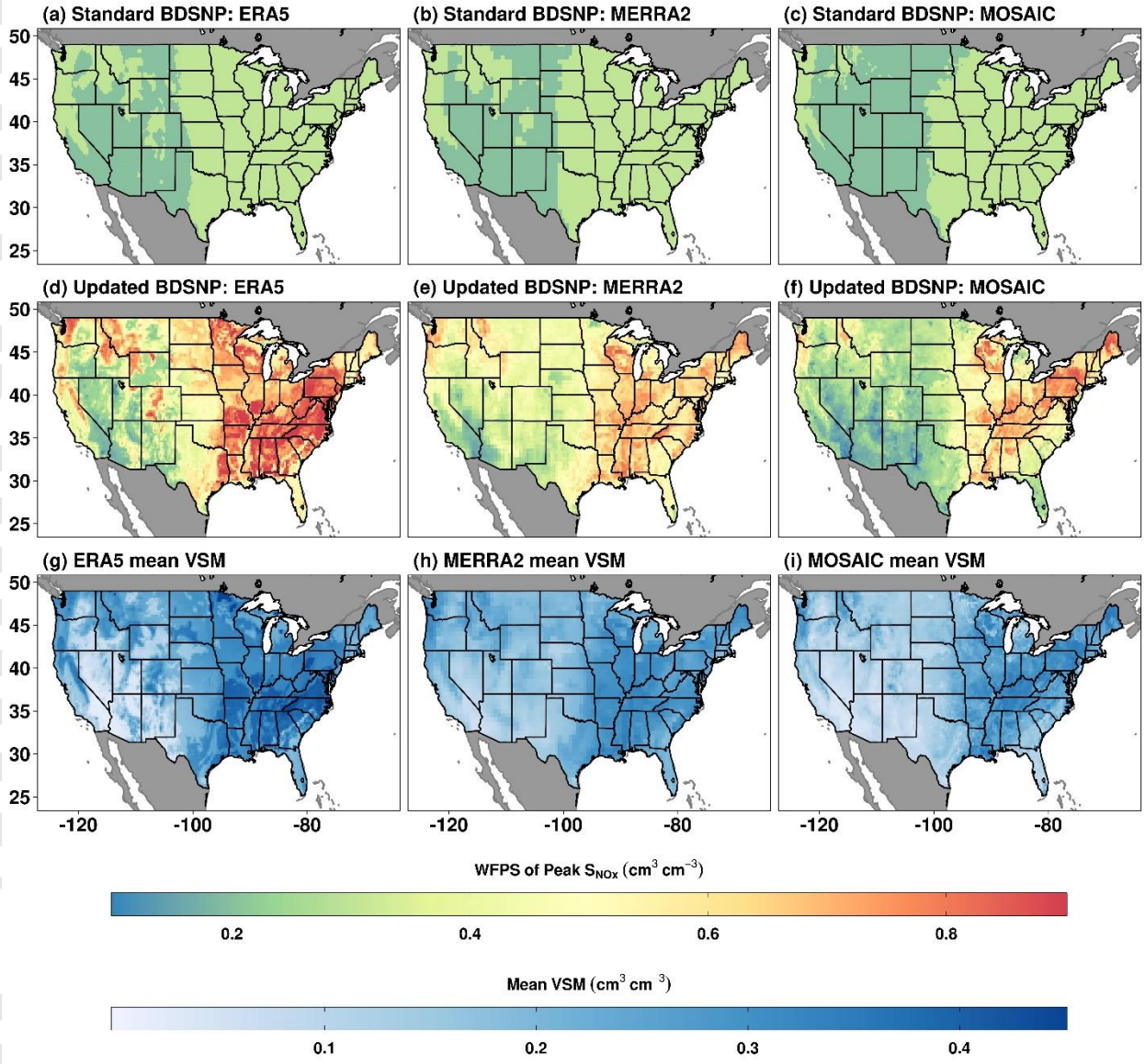


Figure 5: For the three soil moisture products (ERA5-Land, MERRA-2 and NLDAS2-Mosaic), the (a-c) WFPS of peak soil NOx emissions for the standard BDSNP soil moisture function and (d-f) for our updated soil moisture function. (g-i) April-September mean volumetric soil moisture.

model. Our updated parameterization generally increases emissions across the eastern half of the U.S. regardless of the soil moisture product being used, while emissions changes over the western U.S. are more variable and depend on the driving soil moisture product and specific location.

Standard BDNSP emissions show substantial variations spatially when driven by different soil moisture data products (Figs. 6a-c). For example, standard BDSNP emissions driven by Mosaic

This article is protected by copyright. All rights reserved.

Author Manuscript

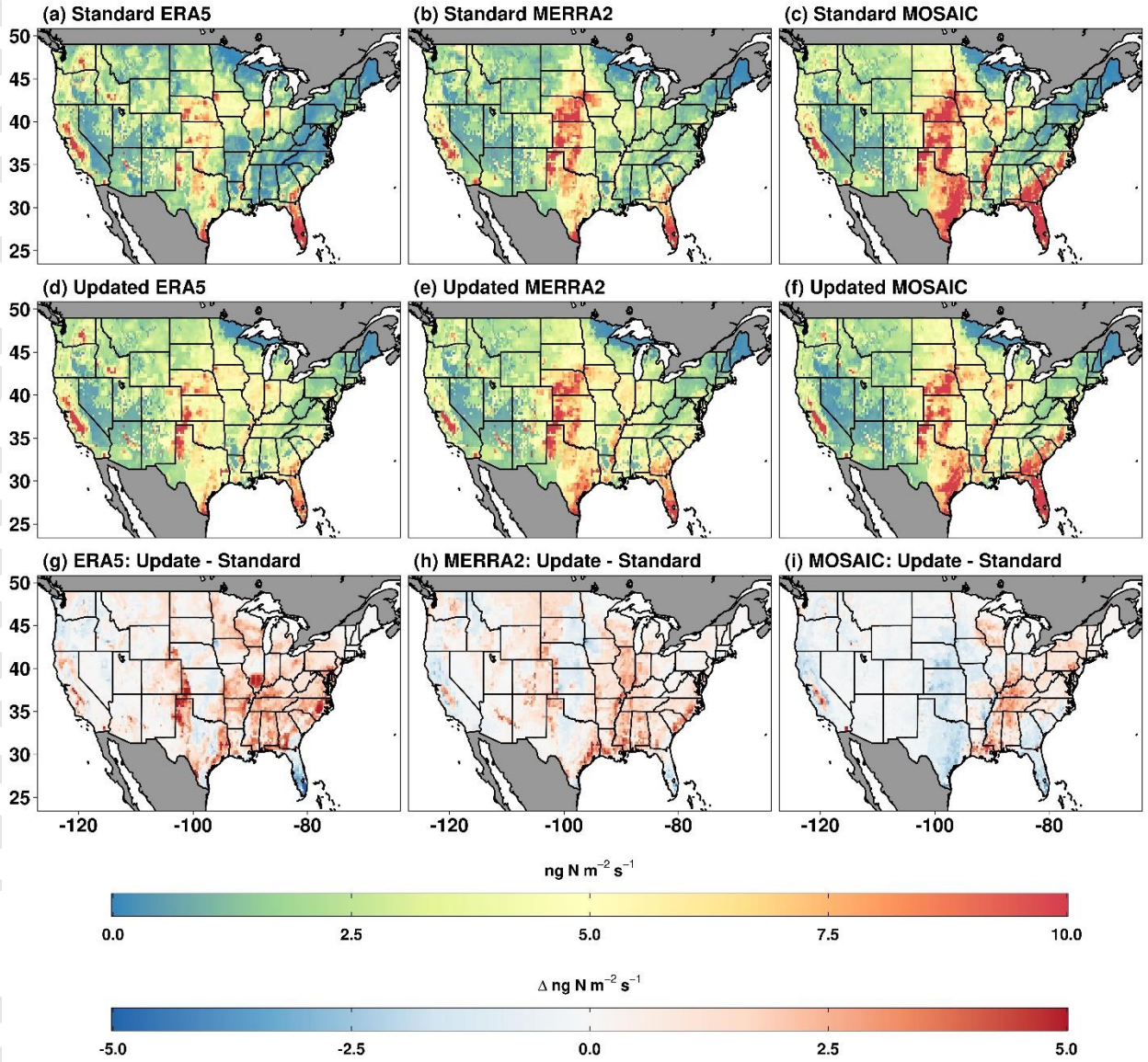


Figure 6: (a-c) Average annual soil NOx emission rates when using the standard BDSNP parameterization and (d-f) when using the updated parameterization. (g-i) The difference between the updated and the standard parameterization. Each column represents a different soil moisture product (ERA5-Land, MERRA-2 and Mosaic).

(Fig. 6c) are up to 41.3% and 23.3% larger than emissions driven by ERA5-Land or MERRA-2 soil moisture, respectively (Figs. 6a-b). These differences are largest in much of the Eastern U.S., including Eastern Texas, The Lower Mississippi River Valley, Central Illinois and Southern Georgia. This is explicitly due to the typical range of modeled soil moisture values within the Mosaic product, which biases much drier than the ERA5-Land or MERRA-2 products. This causes

This article is protected by copyright. All rights reserved.

Author Manuscript

the Mosaic-derived WFPS to more frequently be near the 20% and 30% WFPS optima used in the standard BDSNP, leading to emissions that are scaled higher for a greater fraction of time than the ERA5-Land or MERRA-2 driven emissions. For the updated model (Figs. 6d-f), the spatial emission variations diminish between different soil moisture products. This indicates that using NVSM improves agreement between calculated S_{NOx} emissions, reducing the importance of the soil moisture input. Specifically, for all products, emission hotspots are focused in the Central and Midwestern U.S. with similar spatial patterns observed (Figs. 6 d-f).

The largest differences between the standard and updated parameterization are seen with the ERA5-Land product (Fig. 6g). Given that ERA5-Land soil moisture biases high for most of the Eastern U.S., soil moisture in this region is rarely reduced enough to meet the standard BDSNP non-arid 30% WFPS optimum, leading to emissions that are almost always scaled lower due to near perpetual wet soil conditions (>40% WFPS). When revising to the median NVSM optimum, S_{NOx} increases substantially because the higher optimum value can be easily attained by the ERA5-Land soil moisture (Fig. 5d). S_{NOx} driven by MERRA-2 soil moisture experience the largest increases in the Midwestern and Southeastern U.S., and S_{NOx} driven by Mosaic decrease across much of the Southwestern and Northwestern U.S. due to the soil moisture value of peak emissions shifting slightly higher in the region (Fig. 5f) as well as emissions regularly being scaled lower during very wet and very dry soil conditions in the updated parametrization. For all products, we see decreases in S_{NOx} in Florida, where soil moisture values typically remain close to the standard BDSNP non-arid 30% WFPS optimum, which creates large emission fluxes along the peninsula. The updated parameterization reduces S_{NOx} when soil moisture is at its relative wet and dry extremes, leading to an overall decrease in S_{NOx} there.

This article is protected by copyright. All rights reserved.

Author Manuscript

Comparing different data products with the two parameterizations, the updated parameterization produces more self-consistent emissions estimates regardless of the choice of data input (Figure 7), with r^2 of 0.85 to 0.92 for the updated as compared to 0.56 to 0.75 for the standard parameterizations. We note that the difference in emissions between the standard and updated parameterizations (Figs. 6g-i) and the difference in standard BDSNP emissions when driven by different data products (Fig 7, left column) are of a similar magnitude, again underscoring the role that soil moisture data input plays in determining the magnitude of standard BDSNP S_{NOx}. Spatially, standard BDSNP emissions driven by ERA5-Land are lower in the MW and SE regions than emissions driven by MERRA-2 or Mosaic (Figs. 7a,c). Similarly, standard BDSNP S_{NOx} driven by MERRA-2 are lower in the MW and SE regions than emissions driven by Mosaic. Ultimately, the typical range of modeled soil moisture values largely dictates the magnitude of S_{NOx} when using the standard parametrization. After updating to NVSM, spatial differences between emissions driven by different data products is largely reduced, creating more consistent emissions estimates regardless of the input soil moisture product.

Summed over the contiguous US for the past decade, S_{NOx} are more variable for the standard parameterization, ranging from roughly 0.6 – 1 Tg N yr^{-1} with a decadal mean of 0.82 Tg N yr^{-1} (Figure 8a). The updated parameterization simulates a narrower range in S_{NOx} of 0.85 – .95 Tg N yr^{-1}, with a decadal mean of 0.94 Tg N yr^{-1} (Figure 8b). Notable features in this time series are the response in emissions to the Central US drought in 2012 (Rippey ., 2015) and response to a particularly wet period in the Central U.S. in 2019 toward the start of the growing season (Yin et al. 2020). Standard BDSNP S_{NOx} for 2012 are on average 0.24 Tg N yr^{-1} larger than the decadal average due to drier conditions, which kept soil moisture values closer to the BDSNP optima of 20% and 30% WFPS for a longer period of time and enhancing emissions. However, there is little

This article is protected by copyright. All rights reserved.

Author Manuscript

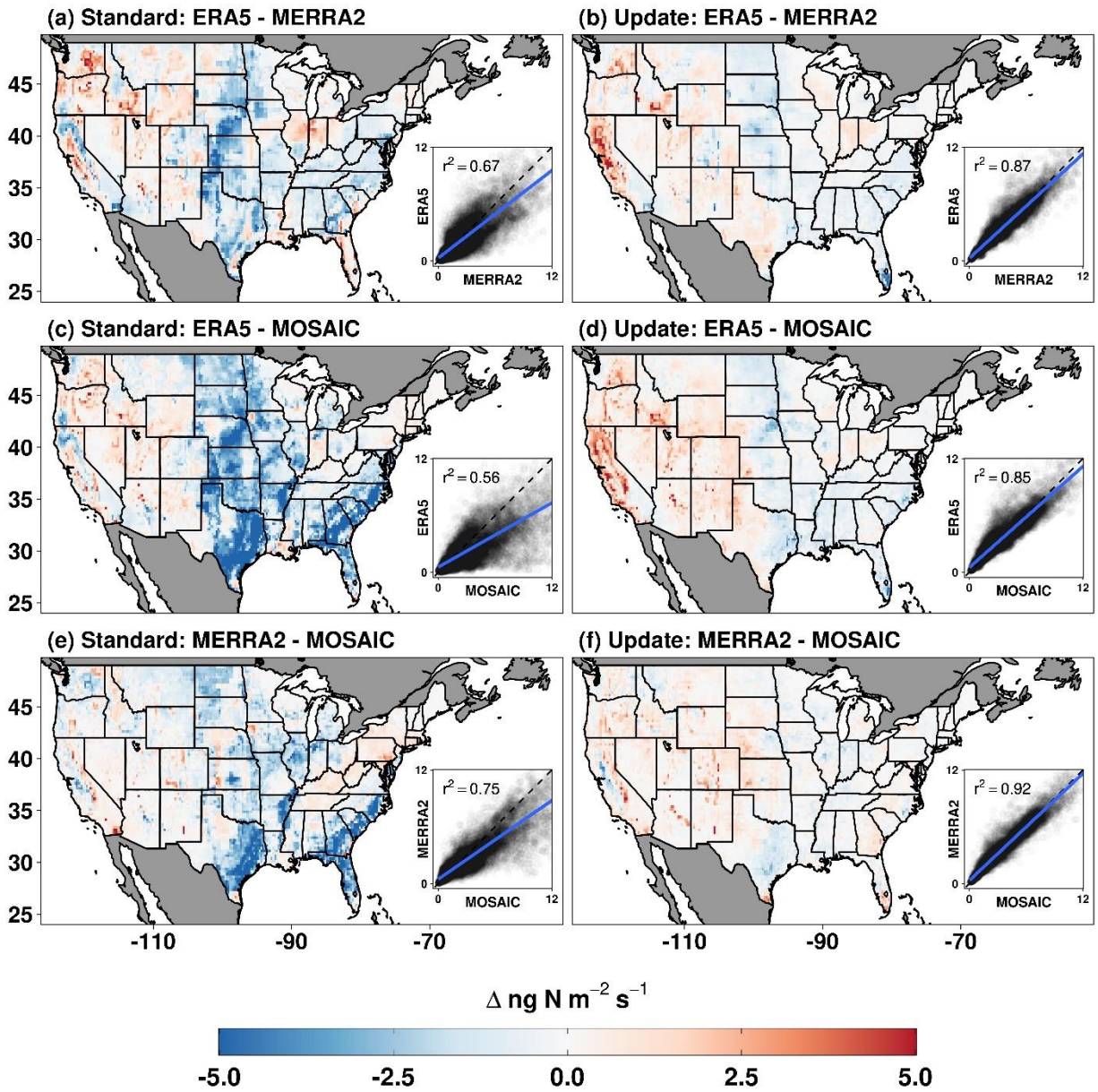


Figure 7: The difference in the annual average soil NOx emission rate when driven by different soil moisture products for the standard BDSNP (left) and updated BDSNP (right). Plot insets at the bottom right of each panel show a scatter plot and best fit line of absolute emission rates for each combination of soil moisture driver, in units of ng N m^2 s^{-1}, with corresponding r^2 values. Each point on the scatter plots represents one pixel from the spatial plots. The panels show (a) standard ERA5-Land – standard MERRA-2, (b) updated ERA5-Land – updated MERRA-2, (c) standard ERA5-Land – standard Mosaic, (d) updated ERA5-Land – updated Mosaic, (e) standard MERRA-2 – standard Mosaic, and (e) updated MERRA-2 – updated Mosaic.

evidence in the literature to suggest that such prolonged dry conditions when soil moisture is at its extreme driest conditions would result in prolonged enhanced S_{NOx}. Likewise, standard BDSNP

This article is protected by copyright. All rights reserved.

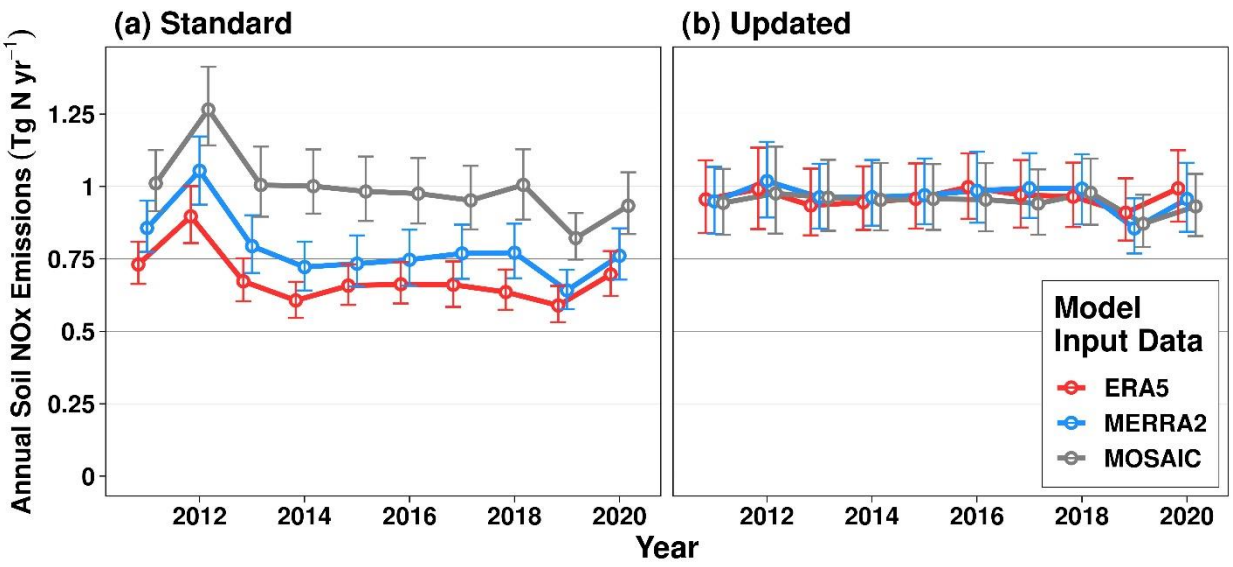


Figure 8: Annual summed soil NOx emissions (Tg N yr^{-1}) for the contiguous U.S. between 2011 and 2020 for (a) the standard BDSNP and (b) the updated BDSNP when driven by different soil moisture products. Error bars represent the 95% confidence interval.

S_{NOx} for 2019 are reduced on average by 0.14 Tg N yr^{-1} compared to the decadal mean, because much of the central U.S. experienced much larger than average rainfall near the start of the growing season (Yin et al., 2020) that elevated soil moisture significantly above the 20% and 30% WFPS optima. In the updated BDSNP, S_{NOx} deviations are reduced in 2012 and 2019 (Fig. 8b), suggesting that the updated parameterization is less sensitive to soil moisture extremes. On average, the multi-model average annual emissions increased by 14.9% across the U.S after applying the updated parametrization. The confidence intervals in Figure 8 do not account for biases across inputs, and the uncertainty range for each model simulation is relative to the specific input data used.

The contribution of soil NOx pulsing to overall emissions in the standard parameterization when driven by Mosaic soil moisture is roughly double that when driven by the ERA5-Land or MERRA-2 soil moisture products. This results in the Mosaic product producing the largest annual emissions estimates for the standard parametrization of the three soil moisture products (Fig. 8a). The dry bias of Mosaic soil moisture relative to ERA5-Land and MERRA-2 results in the pulsing criteria (VSM < 17.5%) being met more frequently, leading to larger pulsing contributions. This

This article is protected by copyright. All rights reserved.

Author Manuscript

leads to a higher frequency and broader spatial extent of soil NOx pulsing in the Mosaic emissions estimate. After applying the revised soil moisture threshold using NVSM, the dry bias of the Mosaic product is largely removed, resulting in pulsing criteria being met more regularly for all three soil moisture products (Fig. 8b).

5. Discussion and Conclusions

In this work, we updated the soil moisture function within the BDSNP S_{NOx} model to produce peak S_{NOx} across a wider range of possible soil moisture conditions than currently implemented in the standard model. Our soil moisture function update has S_{NOx} peak at a unique soil moisture value for each grid cell, no longer uses explicit arid and non-arid soil to determine the moisture optima for peak emissions, and uses normalized volumetric soil moisture in place of water-filled pore space as the soil moisture metric. We additionally revised the soil moisture threshold criteria related to soil NOx pulsing, using NVSM as the soil moisture metric and allowing the threshold value to vary based on data product and at each grid cell. We ran the standard and updated BDSNP for the contiguous U.S. for the years 2011-2020 and compared emissions estimates when driving the model by a variety of different soil moisture products.

The updated parameterization simulates the largest S_{NOx} in agriculturally productive regions across the U.S., as has been found in previous studies. The BDSNP is the default soil NOx parameterization used in the GEOS-Chem model, which uses MERRA-2 meteorological data as inputs (Gelaro et al., 2017). Previous GEOS-Chem studies utilizing MERRA-2 to evaluate S_{NOx} over the contiguous U.S. have produced a similar spatial distribution of emissions as our results (Figure 6b) when using the standard parameterization driven by MERRA-2 (Wang et al. 2021). Our update most notably increases emissions in non-arid regions of the eastern U.S., which typically have wetter soil conditions and experience year-round precipitation, including much of

This article is protected by copyright. All rights reserved.

Author Manuscript

the heavily agricultural Corn Belt region. These results support previous work that suggests wet regions in the eastern U.S. can produce larger S_{NOx} than previously thought and that significant S_{NOx} need not be confined to drier regions (Hall et al. 2018). Multi-model average S_{NOx} for the contiguous U.S. increased by 14.9% after applying our update, with the largest increases in emissions observed in the Southeastern and Midwestern U.S. By using NVSM in the updated parameterization, we no longer need to know soil porosity, removing an additional source of uncertainty from emissions estimates. Further, by removing the static arid vs. non arid approach, the updated parameterization provides a more dynamic path forward for modeling soil NOx emissions.

With the standard BDSNP, the choice of soil moisture input is largely responsible for determining the final magnitude of emissions at any given location, with large discrepancies observed between emissions estimates driven by different soil moisture products. Emissions driven by different soil moisture products were better correlated after implementing our updated parameterization, with R^2 values improving in all cases to approximately 0.9. Soil moisture is a critical control on S_{NOx}, however the representation of modeled soil moisture from different reanalysis products remains inconsistent. Given this circumstance, our updated model parameterization enables not only the representation of S_{NOx} to be improved by more accurately capturing the dynamics of peak emissions at different soil moisture levels for different locations, but also provides an emissions model that is insensitive to choice of input soil moisture product, providing a more consistent and robust baseline for exploring emissions and impacts of S_{NOx}.

All models of soil nitrogen emissions are fundamentally limited by the quality of input of biogeochemical drivers. Our approach here reduces the impact of soil moisture product choice and soil porosity, however improved observational constraints of soil moisture to better capture soil

This article is protected by copyright. All rights reserved.

Author Manuscript

moisture dynamics at finer spatiotemporal scales will further improve models of S_{NOx}. Soil nitrogen availability, and the additional N inputs from human activities, remain a major control of emissions for which there is little observational constraint. Perhaps most valuable to evaluation of both input data and model parameterizations would be further landscape scale (~10's km) observational constraint and evaluation of soil NOx emissions. This requires coupling the updated S_{NOx} framework presented here with a chemical transport model to allow for evaluation with ground-based atmospheric observation of NO and NO_2 and satellite-derived NO_2 column concentrations, which is the focus of future work. While current availability of observational constraints is sparse at this scale, advances and improvements in remote sensing's ability to see S_{NOx} from space (Huber et al., 2020) indicate there is a growing set of observations that can be used to challenge and improve S_{NOx} models.

Acknowledgements

This work was funded by National Aeronautics and Space Administration grant 80NSSC20K0929.

Data Availability Statement

ERA5-Land data can be downloaded from the Copernicus Climate Change Service (C3S) Climate Data Store (CDS) (Muñoz-Sabater, 2019). MERRA-2 and NLDAS2 Mosaic data can be downloaded from the Goddard Earth Sciences Data and Information Services Center (Global Modeling and Assimilation Office (GMAO), 2015; Xia et al., 2012). The TREND-Nitrogen dataset can be accessed from the PANGAEA open access library (Byrnes et al., 2020). The MIrAD-US irrigation dataset can be accessed from the USGS ScienceBase catalog (Brown et al., 2019). Monthly averaged soil NOx emissions output produced with the updated parameterization are available via the University of Michigan Deep Blue Data repository (Huber, 2023).

This article is protected by copyright. All rights reserved.

Author Manuscript

Author Manuscript

References

Almaraz, M., Bai, E., Wang, C., Trousdell, J., Conley, S., Faloona, I., & Houlton, B. Z. (2018). Agriculture is a major source of NOx pollution in California. Science Advances, 4(1), eaao3477. https://doi.org/10.1126/sciadv.aao3477

Andrews, H. M., Homyak, P. M., Oikawa, P. Y., Wang, J., & Jenerette, G. D. (2022). Water-conscious management strategies reduce per-yield irrigation and soil emissions of CO2, N2O, and NO in high-temperature forage cropping systems. *Agriculture, Ecosystems & Environment*, *332*, 107944. https://doi.org/10.1016/J.AGEE.2022.107944

Beck, H. E., Pan, M., Miralles, D. G., Reichle, R. H., Dorigo, W. A., Hahn, S., Sheffield, J., Karthikeyan, L., Balsamo, G., Parinussa, R. M., van Dijk, A. I. J. M., Du, J., Kimball, J. S., Vergopolan, N., & Wood, E. F. (2021). Evaluation of 18 satellite- And model-based soil moisture products using in situ measurements from 826 sensors. *Hydrology and Earth System Sciences*, *25*(1), 17–40. https://doi.org/10.5194/HESS-25-17-2021

Bell, J. E., Palecki, M. A., Baker, C. B., Collins, W. G., Lawrimore, J. H., Leeper, R. D., Hall, M. E., Kochendorfer, J., Meyers, T. P., Wilson, T., & Diamond, H. J. (2013). U.S. Climate Reference Network Soil Moisture and Temperature Observations. *Journal of Hydrometeorology*, *14*(3), 977–988. https://doi.org/10.1175/JHM-D-12-0146.1

Brown, J.F., Howard, D.M., Shrestha, D., and Benedict, T.D. (2019). Moderate Resolution Imaging Spectroradiometer (MODIS) Irrigated Agriculture Datasets for the Conterminous United States (MIrAD-US): U.S. Geological Survey data release [Dataset]. https://doi.org/10.5066/P9NA3EO8

Byrnes, D. K., Van Meter, K. J., & Basu, N. B. (2020). Long-Term Shifts in U.S. Nitrogen Sources and Sinks Revealed by the New TREND-Nitrogen Data Set (1930–2017). *Global Biogeochemical Cycles*, *34*(9). https://doi.org/10.1029/2020GB006626

Byrnes, D.K., Van Meter, K.J., Basu, N.B. (2020). Trajectories Nutrient Dataset for Nitrogen (TREND-nitrogen) [Dataset]. PANGAEA, https://doi.org/10.1594/PANGAEA.917583

Davidson, E. A. (1993). Soil Water Content and the Ratio of Nitrous Oxide to Nitric Oxide Emitted from Soil. *Biogeochemistry of Global Change*, 369–386. https://doi.org/10.1007/978-1-4615-2812-8_20

Duncan, B. N., Yoshida, Y., Olson, J. R., Sillman, S., Martin, R. V., Lamsal, L., Hu, Y., Pickering, K. E., Retscher, C., Allen, D. J., & Crawford, J. H. (2010). Application of OMI observations to a space-based indicator of NOx and VOC controls on surface ozone formation. *Atmospheric Environment*, *44*(18), 2213–2223. https://doi.org/10.1016/J.ATMOSENV.2010.03.010

Eberwein, J. R., Homyak, P. M., Carey, C. J., Aronson, E. L., & Jenerette, G. D. (2020). Large nitrogen oxide emission pulses from desert soils and associated microbiomes. Biogeochemistry, 1–12. https://doi.org/10.1007/s10533-020-00672-9

Famiglietti, J. S., Ryu, D., Berg, A. A., Rodell, M., Jackson, T. J., Famiglietti, C. :, Ryu, D., Berg, A. A., Rodell, M., & Jackson, T. J. (2008). Field observations of soil moisture variability across scales. *Water Resources Research*, *44*(1).

This article is protected by copyright. All rights reserved.

https://doi.org/10.1029/2006WR005804

Forastiere, F., & Peters, A. (2021). Invited Perspective: The NO2 and Mortality Dilemma Solved? Almost There! *Environmental Health Perspectives*, *129*(12). https://doi.org/10.1289/EHP10286

Gasche, R., & Papen, H. (1999). A 3-year continuous record of nitrogen trace gas fluxes from untreated and limed soil of a N-saturated spruce and beech forest ecosystem in Germany: 2. NO and NO2 fluxes. *Journal of Geophysical Research: Atmospheres*, *104*(D15), 18505–18520. https://doi.org/10.1029/1999JD900294

Geddes, J. A., Pusede, S. E., & Wong, A. Y. H. (2022). Changes in the Relative Importance of Biogenic Isoprene and Soil NOx Emissions on Ozone Concentrations in Nonattainment Areas of the United States. *Journal of Geophysical Research: Atmospheres*, *127*(13), e2021JD036361. https://doi.org/10.1029/2021JD036361

Gelaro, R., McCarty, W., Suárez, M. J., Todling, R., Molod, A., Takacs, L., Randles, C. A., Darmenov, A., Bosilovich, M. G., Reichle, R., Wargan, K., Coy, L., Cullather, R., Draper, C., Akella, S., Buchard, V., Conaty, A., da Silva, A. M., Gu, W., … Zhao, B. (2017). The Modern-Era Retrospective Analysis for Research and Applications, Version 2 (MERRA-2). *Journal of Climate*, *30*(14), 5419–5454. https://doi.org/10.1175/JCLI-D-16-0758.1

Global Modeling and Assimilation Office (GMAO) (2015), MERRA-2 tavg1_2d_lnd_Nx: 2d,1-Hourly, Time-Averaged, Single-Level, Assimilation, Land Surface Diagnostics V5.12.4 [Dataset]. Greenbelt, MD, USA, Goddard Earth Sciences Data and Information Services Center (GES DISC), Accessed: 04-04-2022. doi.org/10.5067/RKPHT8KC1Y1T

Hall, S. J., Reyes, L., Huang, W., & Homyak, P. M. (2018). Wet Spots as Hotspots: Moisture Responses of Nitric and Nitrous Oxide Emissions From Poorly Drained Agricultural Soils. *Journal of Geophysical Research: Biogeosciences*, *123*(12), 3589–3602. https://doi.org/10.1029/2018JG004629

Hauglustaine, D. A., Balkanski, Y., & Schulz, M. (2014). A global model simulation of present and future nitrate aerosols and their direct radiative forcing of climate. *Atmospheric Chemistry and Physics*, *14*(20), 11031–11063. https://doi.org/10.5194/ACP-14-11031-2014

Huang, K., Su, C., Liu, D., Duan, Y., Kang, R., Yu, H., Liu, Y., Li, X., Gurmesa, G. A., Quan, Z., Christiansen, J. R., Zhu, W., & Fang, Y. (2022). A strong temperature dependence of soil nitric oxide emission from a temperate forest in Northeast China. *Agricultural and Forest Meteorology*, *323*, 109035. https://doi.org/10.1016/J.AGRFORMET.2022.109035

Huber, D. E., Steiner, A. L., & Kort, E. A. (2020). Daily Cropland Soil NOx Emissions Identified by TROPOMI and SMAP. *Geophysical Research Letters*, *47*(22). https://doi.org/10.1029/2020GL089949

Huber, D. E. (2023). Sensitivity of Modeled Soil NOx Emissions to Soil Moisture: Data [Dataset]. University of Michigan - Deep Blue Data. https://doi.org/10.7302/0r9s-8b54

Hudman, R. C., Moore, N. E., Mebust, A. K., Martin, R. V., Russell, A. R., Valin, L. C., & Cohen, R. C. (2012). Steps towards a mechanistic model of global soil nitric oxide emissions: implementation and space based-constraints. *Atmospheric Chemistry and*

This article is protected by copyright. All rights reserved.

Author Manuscript

Physics, *12*(16), 7779–7795. https://doi.org/10.5194/acp-12-7779-2012

Jafari M, Tavili A, Panahi F, Esfahan EZ, & Ghorbani M. (2018). Reclamation of Arid Lands. In U. Förstner, W. H. Rulkens, & W. Salomons (Eds.), *Reclamation of Arid Lands* (1st ed.). Springer Cham. https://doi.org/https://doi.org/10.1007/978-3-319-54828-9

Jiang, Z., Zhu, R., Miyazaki, K., McDonald, B. C., Klimont, Z., Zheng, B., Folkert Boersma, K., Zhang, Q., Worden, H., Worden, J. R., Henze, D. K., A Jones, D. B., Denier van der Gon, H. A., & Eskes, H. (2022). Decadal variabilities in tropospheric nitrogen oxides over United States, Europe, and China. *Journal of Geophysical Research Atmospheres*. https://doi.org/10.1029/2021JD035872

Ke, P., Kang, R., Avery, L. K., Zhang, J., Yu, Q., Xie, D., & Duan, L. (2021). Temporal variations of soil NO and NO 2 fluxes in two typical subtropical forests receiving contrasting rates of N deposition. *Environmental Pollution*, *295*. https://doi.org/10.1016/j.envpol.2021.118696

Koster, R. D., & Suarez, M. J. (1992). Modeling the land surface boundary in climate models as a composite of independent vegetation stands. *Journal of Geophysical Research: Atmospheres*, *97*(D3), 2697–2715. https://doi.org/10.1029/91JD01696

Laville, P., Lehuger, S., Loubet, B., Chaumartin, F., & Cellier, P. (2011). Effect of management, climate and soil conditions on N2O and NO emissions from an arable crop rotation using high temporal resolution measurements. *Agricultural and Forest Meteorology*, *151*(2), 228–240. https://doi.org/10.1016/j.agrformet.2010.10.008

Li, M., Wu, P., & Ma, Z. (2020). A comprehensive evaluation of soil moisture and soil temperature from third-generation atmospheric and land reanalysis data sets. *International Journal of Climatology*, *40*(13), 5744–5766. https://doi.org/10.1002/JOC.6549

Lu, X., Ye, X., Zhou, M., Zhao, Y., Weng, H., Kong, H., Li, K., Gao, M., Zheng, B., Lin, J., Zhou, F., Zhang, Q., Wu, D., Zhang, L., & Zhang, Y. (2021). The underappreciated role of agricultural soil nitrogen oxide emissions in ozone pollution regulation in North China. *Nature Communications 2021 12:1*, *12*(1), 1–9. https://doi.org/10.1038/s41467-021-25147-9

Maljanen, M., Martikkala, M., Koponen, H. T., Virkajärvi, P., & Martikainen, P. J. (2007). Fluxes of nitrous oxide and nitric oxide from experimental excreta patches in boreal agricultural soil. *Soil Biology and Biochemistry*, *39*(4), 914–920. https://doi.org/10.1016/J.SOILBIO.2006.11.001

Miyazaki, K., Bowman, K., Sekiya, T., Eskes, H., Boersma, F., Worden, H., Livesey, N., Payne, V. H., Sudo, K., Kanaya, Y., Takigawa, M., & Ogochi, K. (2020). Updated tropospheric chemistry reanalysis and emission estimates, TCR-2, for 2005–2018. *Earth System Science Data*, *12*(3), 2223–2259. https://doi.org/10.5194/essd-12-2223-2020

Muñoz-Sabater, J., Dutra, E., Agustí-Panareda, A., Albergel, C., Arduini, G., Balsamo, G., Boussetta, S., Choulga, M., Harrigan, S., Hersbach, H., Martens, B., Miralles, D. G., Piles, M., Rodríguez-Fernández, N. J., Zsoter, E., Buontempo, C., & Thépaut, J. N. (2021). ERA5-Land: A state-of-the-art global reanalysis dataset for land applications. *Earth System Science Data*, *13*(9), 4349–4383. Accessed: 04-13-2022. https://doi.org/10.5194/ESSD-13-

This article is protected by copyright. All rights reserved.

Author Manuscript

Author Manuscript

4349-2021

Muñoz-Sabater, J., (2019): ERA5-Land hourly data from 1981 to present [Dataset]. Copernicus Climate Change Service (C3S) Climate Data Store (CDS). Accessed: 04-04-2022. https://doi.org/10.24381/cds.e2161bac

Mushinski, R. M., Payne, Z. C., Raff, J. D., Craig, M. E., Pusede, S. E., Rusch, D. B., White, J. R., & Phillips, R. P. (2020). Nitrogen cycling microbiomes are structured by plant mycorrhizal associations with consequences for nitrogen oxide fluxes in forests. *Global Change Biology*, *27*(5), 1068–1082. https://doi.org/10.1111/GCB.15439

Oikawa, P. Y., Ge, C., Wang, J., Eberwein, J. R., Liang, L. L., Allsman, L. A., Grantz, D. A., & Jenerette, G. D. (2015). Unusually high soil nitrogen oxide emissions influence air quality in a high-temperature agricultural region. *Nature Communications*, *6*(1), 1–10. https://doi.org/10.1038/ncomms9753

Pervez, M. S., & Brown, J. F. (2010). Mapping Irrigated Lands at 250-m Scale by Merging MODIS Data and National Agricultural Statistics. Remote Sensing 2010, Vol. 2, Pages 2388-2412, 2(10), 2388–2412. https://doi.org/10.3390/RS2102388

Pilegaard, K. (2013). Processes regulating nitric oxide emissions from soils. *Philosophical Transactions of the Royal Society B: Biological Sciences*, *368*(1621), 20130126. https://doi.org/10.1098/rstb.2013.0126

Qu, Z., Jacob, D. J., Silvern, R. F., Shah, V., Campbell, P. C., Valin, L. C., & Murray, L. T. (2021). US COVID-19 shutdown demonstrates importance of background NO_2 in inferring NO_x emissions from satellite NO_2 observations. *Geophysical Research Letters*, e2021GL092783. https://doi.org/10.1029/2021GL092783

Rasool, Q. Z., Zhang, R., Lash, B., Cohan, D. S., Cooter, E. J., Bash, J. O., & Lamsal, L. N. (2016). Enhanced representation of soil NO emissions in the Community Multiscale Air Quality (CMAQ) model version 5.0.2. *Geoscientific Model Development*, *9*(9), 3177–3197. https://doi.org/10.5194/gmd-9-3177-2016

Reichle, R. H., De Lannoy, G. J. M., Liu, Q., Ardizzone, J. V., Colliander, A., Conaty, A., Crow, W., Jackson, T. J., Jones, L. A., Kimball, J. S., Koster, R. D., Mahanama, S. P., Smith, E. B., Berg, A., Bircher, S., Bosch, D., Caldwell, T. G., Cosh, M., González-Zamora, Á., … Zeng, Y. (2017). Assessment of the SMAP Level-4 surface and root-zone soil moisture product using in situ measurements. *Journal of Hydrometeorology*, *18*(10), 2621–2645. https://doi.org/10.1175/JHM-D-17-0063.1

Rippey, B. R. (2015). The U.S. drought of 2012. *Weather and Climate Extremes*, *10*, 57–64. https://doi.org/10.1016/J.WACE.2015.10.004

Schaefer, G. L., Cosh, M. H., & Jackson, T. J. (2007). The USDA Natural Resources Conservation Service Soil Climate Analysis Network (SCAN). *Journal of Atmospheric and Oceanic Technology*, *24*(12), 2073–2077. https://doi.org/10.1175/2007JTECHA930.1

Schaufler, G., Kitzler, B., Schindlbacher, A., Skiba, U., Sutton, M. A., & Zechmeister-Boltenstern, S. (2010). Greenhouse gas emissions from European soils under different land use: effects of soil moisture and temperature. *European Journal of Soil Science*, *61*(5), 683–

This article is protected by copyright. All rights reserved.

696. https://doi.org/10.1111/J.1365-2389.2010.01277.X

Schindlbacher, A., & Zechmeister-Boltenstern, S. (2004). Effects of soil moisture and temperature on NO, NO2 , and N2O emissions from European forest soils. *Journal of Geophysical Research*, *109*(D17), D17302. https://doi.org/10.1029/2004JD004590

Sha, T., Ma, X., Zhang, H., Janechek, N., Wang, Y., Wang, Y., Castro García, L., Jenerette, G. D., & Wang, J. (2021). Impacts of Soil NOx Emission on O3 Air Quality in Rural California. *Environmental Science & Technology*, acs.est.0c06834. https://doi.org/10.1021/acs.est.0c06834

Silvern, R. F., Jacob, D. J., Mickley, L. J., Sulprizio, M. P., Travis, K. R., Marais, E. A., Cohen, R. C., Laughner, J. L., Choi, S., Joiner, J., & Lamsal, L. N. (2019). Using satellite observations of tropospheric NO2 columns to infer long-term trends in US NO x emissions: the importance of accounting for the free tropospheric NO2 background. *Atmos. Chem. Phys*, *19*, 8863–8878. https://doi.org/10.5194/acp-19-8863-2019

Steinkamp, J., & Lawrence, M. G. (2011). Improvement and evaluation of simulated global biogenic soil NO emissions in an AC-GCM. Atmos. Chem. Phys, 11, 6063–6082. https://doi.org/10.5194/acp-11-6063-2011

Su, C., Zhu, W., Kang, R., Quan, Z., Liu, D., Huang, W., Shi, Y., Chen, X., & Fang, Y. (2021). Interannual and seasonal variabilities in soil NO fluxes from a rainfed maize field in the Northeast China. *Environmental Pollution*, *286*, 117312. https://doi.org/10.1016/j.envpol.2021.117312

Szukics, U., Abell, G. C. J., Hödl, V., Mitter, B., Sessitsch, A., Hackl, E., & Zechmeister-Boltenstern, S. (2010). Nitrifiers and denitrifiers respond rapidly to changed moisture and increasing temperature in a pristine forest soil. *FEMS Microbiology Ecology*, *72*(3), 395–406. https://doi.org/10.1111/J.1574-6941.2010.00853.X

Van Dijk, S. M., & Duyzer, J. H. (1999). Nitric oxide emissions from forest soils. *Journal of Geophysical Research Atmospheres*, *104*(D13), 15955–15961. https://doi.org/10.1029/1999JD900195

Vinken, G. C. M., Boersma, K. F., Maasakkers, J. D., Adon, M., & Martin, R. V. (2014). Worldwide biogenic soil NO x emissions inferred from OMI NO 2 observations. *Atmos. Chem. Phys*, *14*, 10363–10381. https://doi.org/10.5194/acp-14-10363-2014

Wang, Y., Ge, C., Garcia, L. C., Jenerette, G. D., Oikawa, P. Y., & Wang, J. (2021). Improved modelling of soil NOx emissions in a high temperature agricultural region: role of background emissions on NO2 trend over the US. *Environmental Research Letters*, *16*(8), 084061. https://doi.org/10.1088/1748-9326/AC16A3

Weng, H., Lin, J., Martin, R., Millet, D. B., Jaeglé, L., Ridley, D., Keller, C., Li, C., Du, M., & Meng, J. (2020). Global high-resolution emissions of soil NOx, sea salt aerosols, and biogenic volatile organic compounds. Scientific Data 2020 7:1, 7(1), 1–15. https://doi.org/10.1038/s41597-020-0488-5

Xia, Y., et al. (2012). NCEP/EMC (2009), NLDAS Mosaic Land Surface Model L4 Hourly 0.125 x 0.125 degree V002 [Dataset]. NASA/GSFC/HSL, Greenbelt, Maryland, USA,

This article is protected by copyright. All rights reserved.

Author Manuscript

Goddard Earth Sciences Data and Information Services Center (GES DISC), Accessed: 04-04-2022. doi.org/10.5067/EN4MBWTCENE5

Yao, Z., Wu, X., Wolf, B., Dannenmann, M., Butterbach-Bahl, K., Brüggemann, N., Chen, W., & Zheng, X. (2010). Soil-atmosphere exchange potential of NO and N2O in different land use types of Inner Mongolia as affected by soil temperature, soil moisture, freeze-thaw, and drying-wetting events. *Journal of Geophysical Research Atmospheres*, *115*(17). https://doi.org/10.1029/2009JD013528

Yienger, J. J., & Levy, H. (1995). Empirical model of global soil-biogenic NOx emissions. *Journal of Geophysical Research*, *100*(D6), 11447. https://doi.org/10.1029/95JD00370

Yin, Y., Byrne, B., Liu, J., Wennberg, P. O., Davis, K. J., Magney, T., Köhler, P., He, L., Jeyaram, R., Humphrey, V., Gerken, T., Feng, S., Digangi, J. P., & Frankenberg, C. (2020). Cropland Carbon Uptake Delayed and Reduced by 2019 Midwest Floods. *AGU Advances*, *1*(1), e2019AV000140. https://doi.org/10.1029/2019av000140

Zaussinger, F., Dorigo, W., Gruber, A., Tarpanelli, A., Filippucci, P., & Brocca, L. (2019). Estimating irrigation water use over the contiguous United States by combining satellite and reanalysis soil moisture data. Hydrology and Earth System Sciences, 23(2), 897–923. https://doi.org/10.5194/HESS-23-897-2019

Zhou, Z., Zheng, X., Xie, B., Liu, C., Song, T., Han, S., & Zhu, J. (2010). Nitric oxide emissions from rice-wheat rotation fields in eastern China: Effect of fertilization, soil water content, and crop residue. *Plant and Soil*, *336*(1), 87–98. https://doi.org/10.1007/S11104-010-0450-Y/FIGURES/3

Zörner, J., Penning De Vries, M., Beirle, S., Sihler, H., Veres, P. R., Williams, J., & Wagner, T. (2016). Multi-satellite sensor study on precipitation-induced emission pulses of NOx from soils in semi-arid ecosystems. *Atmospheric Chemistry and Physics*, *16*(14), 9457–9487. https://doi.org/10.5194/acp-16-9457-2016

Wu, Z., Feng, H., He, H., Zhou, J., & Zhang, Y. (2021). Evaluation of Soil Moisture Climatology and Anomaly Components Derived From ERA5-Land and GLDAS-2.1 in China. Water Resources Management, 35(2), 629–643. https://doi.org/10.1007/S11269-020-02743-w

Xu, L., Chen, N., Zhang, X., Moradkhani, H., Zhang, C., & Hu, C. (2021). In-situ and triple-collocation based evaluations of eight global root zone soil moisture products. Remote Sensing of Environment, 254, 112248. https://doi.org/10.1016/J.RSE.2020.112248

Author Manuscript

This article is protected by copyright. All rights reserved.